Global burned area products from remote sensing: an evaluation of fire patch metrics for regional applications in Brazil

Joana Messias Pereira Nogueira [1*],
Julien Ruffault[1],
Emilio Chuvieco[2],
Florent Mouillot[1]

[1] UMR CEFE 5175, CNRS, Université de Montpellier, Université Paul-Valéry Montpellier, EPHE, IRD, 1919 route de Mende, 34293 Montpellier Cedex 5, France; *author corresponding: joananog@yahoo.com.br; julien.ruff@gmail.com; florent.mouillot@ird.fr

[2] Environmental Remote Sensing Research Group, Department of Geography and Geology, University of Alcalá, C/ Colegios 2, 28801 Alcalá de Henares, Spain; emilio.chuvieco@uah.es

Abstract. Global burned area (BA) datasets from remote sensing provide fruitful information for carbon emissions and for Dynamic Global Vegetation Model's (DGVM) benchmarking. Patch level analysis recently emerged as an additional informative feature of the fire regime. We evaluated a step further the ability of global BA products to accurately represent fire patch features, in the fire-prone Brazilian savannas. We used the pixel-level burned area from LANDSAT, MODIS MCD45A1 and the European Space Agency (ESA) fire Climate Change Initiative (FIRE_CCI) for the period 2002-2009 to identify individual fire patches that we compared by linear regressions. Correlations between patch areas showed R^2>0.6 for all comparisons, with a slope of 0.99 between FIRE_CCI and MCD45A1 but a lower slope (0.6 - 0.8) when compared to the LANDSAT data. Shape complexity was less correlated (R^2 = 0.5) between global products, and R^2=0.2 between global products and the LANDSAT data, due to coarser resolution. For the morphological features of the ellipse fitted over fire patches, R^2 reached 0.6 for the ellipse's eccentricity and varied from 0.4 to 0.8 for its azimuthal directional angle. We conclude that global BA products underestimate BA due to missing small fires, but also underestimate patch areas. Patch complexity is the least correlated variable, but ellipse features appear to be reliable information to be further used for quality product assessment, global pyrogeography or DGVM benchmarking.

Keywords: fire ecology, Brazilian savannas, MCD45A1, ESA FIRE_CCI, patch indices
Palavras-chave: ecologia do fogo, Cerrado, MCD45A1, ESA FIRE_CCI, indices de patches

1. Introduction

Fires contribute to the emissions of CO_2 and other greenhouse gases to the atmosphere by combustion process and post-fire decomposition of biomass, with high number of fire events in tropical regions. In the early 2000's, global burned area (BA) datasets from remote sensing emerged to provide monthly gridded data (Mouillot et al., 2014) to quantify the biomass burning and to include fires in global carbon budget, estimated by global biogeochemical models. Recently, embedding fires in dynamic global vegetation models (DGVMs) appeared as a keystone issue to forecast future biosphere/atmosphere interactions under global anthropogenic changes through the biomass combustion process and the indirect effect on vegetation dynamic (Hantson et al., 2016). However, intercomparison of global BA products show significant discrepancies in the total burnt area, its interannual variability and temporal trend (Hantson et al., 2016), being underrepresentation of small fires as a potential bias (Randerson et al., 2002).

The interest in partitioning BA at the grid cell level (usually 0.25°, 0.5° or 1° resolution) into patch size distribution from the pixel-level information (500m-1km resolution) has recently emerged to better characterize a fire regime for pyrogeographic analysis (Hantson et al., 2014). More recently, DGVM benchmarking protocols also used the information on patch distribution as an intermediate validation step before the final burned area but had not been explored due to the lack of data on fire patches at the global scale. Indeed, fire modules in DGVMs actually simulate fire spread as a theoretical fire ellipse (Rothermel, 1972) with an

elongation proportional to wind speed that combined to fire number result in final burned area. At the landscape level, fire elongation has been early identified as an index of the contribution of wind speed to fire spread, but locally modified by topography, vegetation spatial pattern and wind direction (Barros et al., 2014) affecting the fire orientation in the direction of fire spread. In other, the complexity of fire shapes has been identified as a key component of post-fire regeneration of the vegetation, with unburned patches within or at the boundary of large fires being a significant agent of the vegetation recolonization process (Oliveira et al., 2015).

Comparing the spatial organization of pixels spatial arrangement at the landscape level relies on patch metrics that inform the composition of landscapes. This framework has been used in fire ecology to identify key information related to fire drivers and post-fire vegetation dynamic but have, yet, not been assessed in global burnt area products from remote sensing. In this context, we question here how some key patch metrics (area, patch boundary complexity and patch ellipses) describing fire patches at the landscape level with high resolution fire maps (as Landsat images) are conserved when calculated with lower resolution global fire products to provide enough fruitful information at the landscape or regional level, and stimulate its further use for DGVM benchmarking or global pyrogeography. So, we focused our study on a selected site in the Cerrado, comparing a Landsat-based fire patch database and the two mostly used remote sensing products fires assessments (MODIS MCD45A1, and ESA FIRE_CCI).

2. Methodology

2.1. Study area

The study area (30.000 km^2) is a validation study site for the ESA FIRE_CCI BA dataset (Padilla et al., 2015). It is located in the northwestern part of the Tocantins state (TO), from Brazil (Figure 1) at the boundary between the savanna biome (Cerrado) and the Amazonian forest, a fire-prone region as a consequence of a flammable and dry vegetation type, marked by dry season from May to September and with a high human pressure on human ignitions (Viergever, 2009). This region is then highly susceptible to fire risk, with the highest incidence records for years 2005 and 2008 (INPE, 2016).

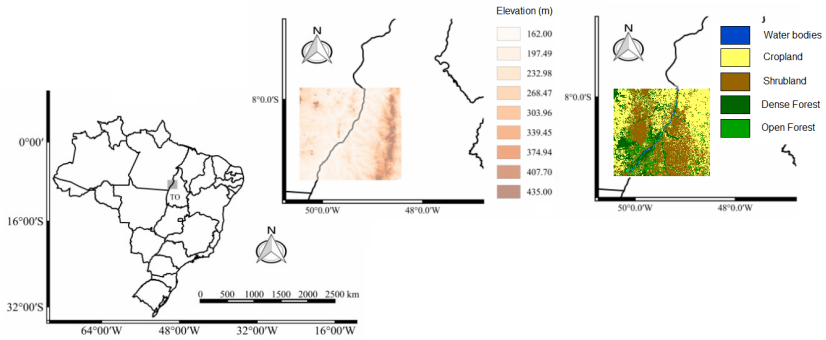

Figure 1. Study area (in gray), located on the North Western part of Tocantins state (TO) (9 ° 57 'S - 7° 57'S to 50 ° 45' - 48°44' W) within Brazil. Elevation and land cover maps (source: SRTM and ESA Land Cover CCI 2005) are also shown

2.2. Burned area (BA) datasets

We selected the most BA datasets used in global fire assessments (Mouillot et al., 2014) derived from different sensors (Table 1). LANDSAT images were processed with the Burnt Area Mapping Software (ABAMS) (Bastarrika et al., 2008) for burned area characterization. MCD45A1 and ESA FIRE_CCI were characterized by a burned date (BD) layer indicating the day of the year when a fire signal occurred, and we selected only the burned dates with confidence level higher than 50%. All the datasets were re-projected at 30m resolution in WGS 84 UTM 22S projection over the Landsat scene path 223 and row 066 (corresponding of study area) of world reference system . The analysis was performed during the fire seasons for temporal series indicated in Table 1 for each BA dataset and all data statistical analysis and processing were developed using the '*raster*' (Hijmans, 2014) and '*sp*' (Pebesma and Bivand, 2005) packages from R program (https://CRAN.R-project.org).

Table 1. Descriptions of global burned area data used in detecting fire patches

Burned area dataset	Satellite[1], sensor	Temporal and spatial resolution	Temporal series used	Reference
LANDSAT	LANDSAT 5, TM LANDSAT 7, ETM+	15 days, 30m	2002-2009	Bastarrika et al., 2011
MCD45A1	TERRA, MODIS	daily, 500m		Roy et al., 2008
ESA FIRE_CCI	ENVISAT, MODIS	daily, 300m	2006-2008	Chuvieco et al., 2016

[1]LANDSAT- Land Remote Sensing Satellite;[1]MODIS - Moderate Resolution Imaging Spectroradiometer;[1]ESAFIRECCI- Medium Resolution Imaging Spectrometer;[3]Fire_cci project - European Space Agency's Fire Climate Change Initiative

2.3. Fire patch identification and metrics

We identified to individual burned patches (ID) from BD dataset of MCD45A1 and ESA FIRE_CCI using a spatio-temporal *flood fill* algorithm (see Archibald and Roy, 2009 for details) with eight days as time interval (cut-off). These ID and BD maps resultants were disaggregated to the spatial resolution of 30m and re-projected to WGS 84 UTM 22S with the nearest neighborhood method for comparison with the LANDSAT dataset, which had fire patches directly identified by ABAMS.

The individual patch description metrics were computed from the yearly patch ID maps, where each burned pixel is referenced by the patch ID it belongs to. For each patch, we calculated its surface area and its core area (both in m^2) corresponding to the surface area of pixels located at a given distance (we chose 500m) inside the external boundary of a patch. Patch shape complexity was evaluated from its shape index calculate as perimeter/area$^{0.5}$ (Figure 2). We performed these patch size and shape metrics using *'SDMtools'* (Vanderwal et al., 2014) package from R. We also computed the ellipse fitting the spatial distribution of burned pixels to capture the directional azimuthal angle (theta) and the elongation of the patch (eccentricity, E) (Figure 2). The patches with same patch ID were converted into points with geographic coordinates corresponding to the center of the pixels, using the '*aspace*' package (Bui et al., 2012) from R to fit the ellipse. E=0 corresponds to the most elongated shape and E=1 to a perfect circle, while theta angle corresponds to the clockwise deviation of the longest axis of the ellipse from the northern direction (Figure 2). These selected indices give information on the size, shape complexity and orientation/direction of the fire patches as proxies of the theoretical fire spread simulated in DGVMs (Rothermel, 1972).

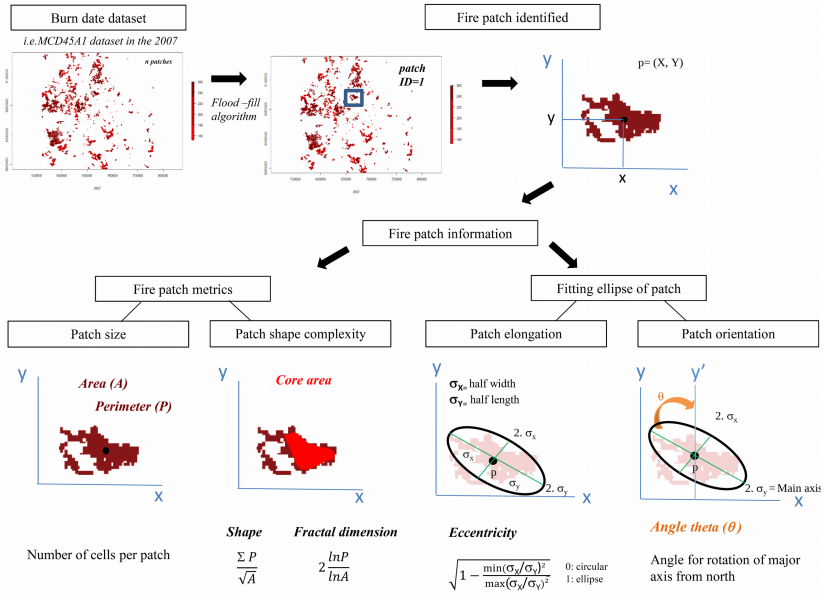

Figure 2. Flowchart of the processing chain of fire patches identification and their metrics of size (area, and core area, shape complexity (shape index), elongation (eccentricity) and orientation (azimuthal angle theta of the longest axis) of the ellipse fitted over the patch

2.4. Data analysis

We compared the different BA products (MCD45A1, LANDSAT, ESA FIRE_CCI) one to each based on their patch features relationships. We first cross tabulated yearly patch ID maps to identify overlapping patches between two sensors. For each patch ID and a given sensor, we obtained the list of the overlapping patch IDs in each of the other sensors, and the percentage of overlapping surface. When a patch in a given sensor overlapped more than one patch in the other sensor, we selected the largest patch. To test for any potential biased comparisons between patches overlapping only over few pixels, we computed the coefficient of determination R^2 using a general linear model (GLM) between overlapping patch surfaces with thresholds of overlap rates (OR%) varying from 10 to 100%. Increasing the OR threshold lead to an increasing R^2 of the patch size correlation for all sensor comparisons.We selected an OR threshold of 30% leading to patch size correlations R^2>0.70 and then computed linear regressions between patches with OR>30% for each patch metric and extracted their R^2, indicating the fraction of the variance explained by the best-fitted linear regression, p-values and slopes to evaluate the significant potential bias to the 1:1 line expected if the sensors are fully conservative of the patch metrics. The GLM and normality of the regression residuals were performed in R program and significant non-normality values ($p<0.01$) were log-transformed (area and core area). We hypothesized that correlations might be dependent on patch size, with boundary uncertainties in global remote sensing BA products affecting more importantly shape indices on small patches. We then performed GLM with the patch size thresholds >90ha, >270ha, >450ha, >630ha and >900ha.

3. Results and Discussion

3.1. Patch metrics correlations

For the patch area (Figure 3A), the highest R^2 (R^2>0.8 for all patch sizes thresholds) and slopes close to 1 were obtained for the ESA FIRE_CCI x MCD45A1, indicating very similar patch sizes between the two global BA products. When comparing global BA products to

LANDSAT, R^2 were also high for ESA FIRE_CCI (R^2>0.8) and a little lower with MCD45A1 (R^2 varies between 0.4 and 0.8). Slopes of the regression for both global BA products ESA FIRE_CCI and MCD45A1 cross-tabulated with LANDSAT varied between 0.8 for all fire size thresholds and 0.6 for larger fire sizes, indicating an underestimation of patch areas of similar magnitude for both global BA products. The correlation coefficients for the core area (Figure 3B) were similar to the total patch area, but with regression slopes reaching (0.6-0.9), indicating a slight lower error in patch areas when removing the patch boundary buffer zone, where uncertainty seems to be the highest. Shape index (Figure 3C) were correlated with R^2 around 0.5 between the two global products ESA FIRE_CCI and MCD45A1 but poorly correlated when compared to LANDSAT (R^2<0.3).

When analyzing the comparison of the fitted ellipse features of eccentricity (Figure 3D) and theta angle (Figure 3E), R^2 were low for all comparisons, but reached values R^2>0.3 for patches larger than 630ha for eccentricity (Figure 3D) and R^2>0.4 for patches larger than 630ha for theta. Below this patch size threshold, R^2 were below 0.5. Slopes of the regressions between eccentricities vary between 0.3 and 0.7 for patches larger than 450ha, lower than the expected 1:1 line, indicating an underestimation of patch elongation and missing pixels at the extremes of patches. Slopes of the regressions for theta varied between 0.7 and 1.1 for all products comparison, close to the expected unbiased 1:1 line.

Our results could point out some discrepancies in global remote sensing BA products regarding fires smaller than 450 ha when compared to the reference fine resolution LANDSAT dataset. On the one hand, the mean annual burned area covered by fire patches smaller than 270ha represents an average 4% to 15% of the total burned area, a value close to the usually assumed 10% of missing burned area due to missing small fires in global BA (Randerson et al., 2012). Beside this missing burned surface in global remote sensing BA products, our results particularly illustrate the little overlap between these small fires (<270ha) derived from different BA products less than 40%. The small fire issue in global BA is now well recognized for most ecosystems, as in Europe where only fires above 500ha have been shown to be accurately captured by global products (Vilar et al., 2015). For Cerrado, we then confirm the same issue as previously observed (Libonati et al., 2015)

Our second main result is the underestimation of patch size for large fires. Our regressions slopes between both global BA products (MCD45A1, ESA FIRE_CCI) with LANDSAT suggest an underestimation by 10 to 40%. For the Cerrado region, a 25% underestimation between MCD45A1 and LANDSAT is observed in Araujo and Ferreira (2015) and up 50 to 60% (Libonati et al., 2015). When using high resolution remotely sensed fire patches, patch size and patch boundary complexity, have been identified as the main explanatory variables for this discrepancy when scaling up from 30m to 1km resolution (Sa et al., 2007). When comparing the mostly used global BA products, all products have been acknowledged to underestimate burned-area and that an increase in pixel size or burned patch elongation, results in larger estimation errors (Anaya and Chuvieco, 2012). This result suggests that correcting the bias on patch sizes obtained from pixel-level global remote sensing according to the slope obtained on test sites across different biomes could be further used for upscaling BA at the 0.5° final products.

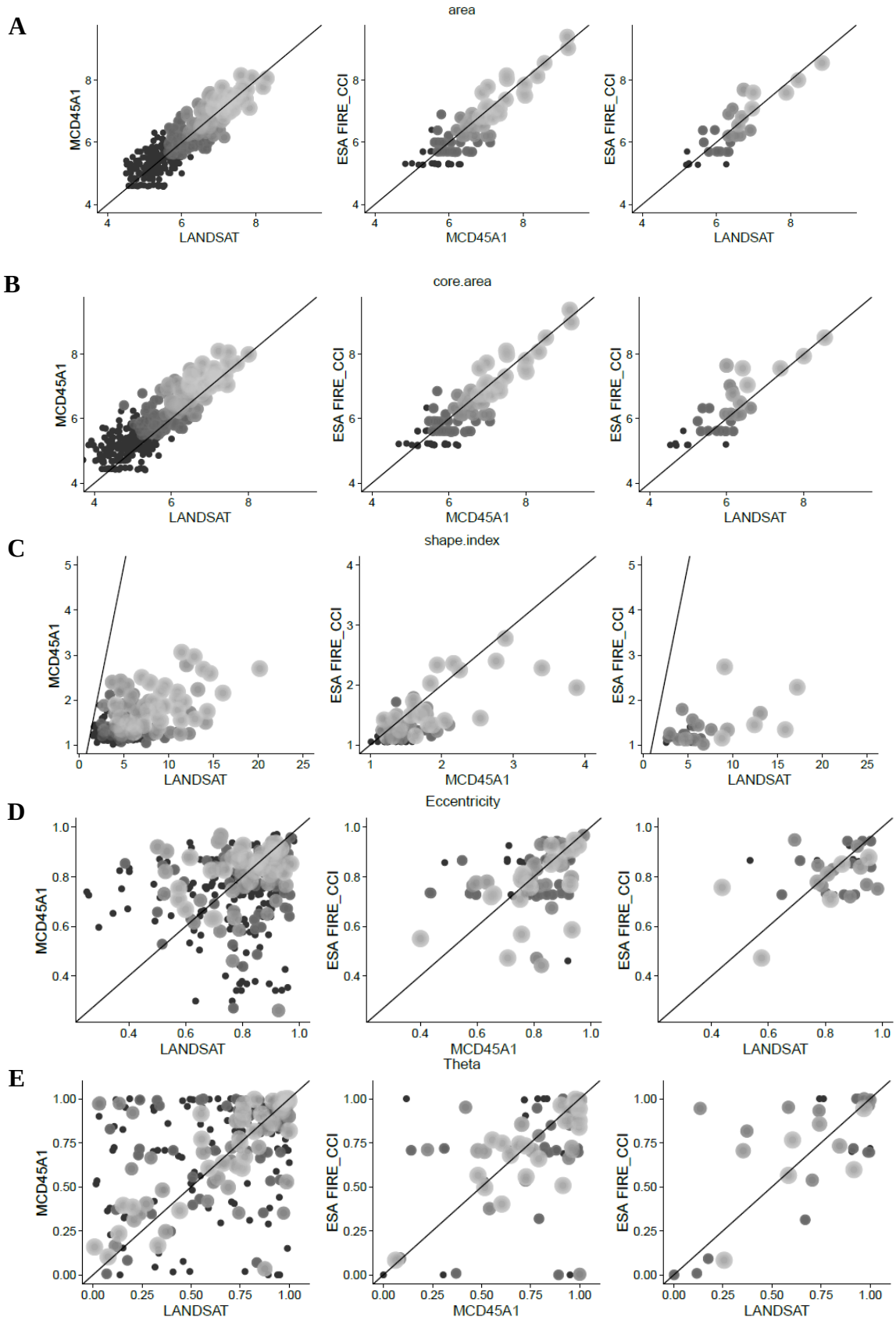

Figure 3. Correlations of the patch metrics: **A**- area (log), **B**- core.area (log), **C**- shape index (unitless) and ellipse fitted over fire patches: **D**- eccentricity (unitless) and **E**- theta angle (sinus), for comparisons (ordering by column): 1- LANDSAT x MCD45A1, 2- MCD45A1 x ESA FIRE_CCI and 3- LANDSAT x ESA FIRE_CCI.

The grey scale colors of individual points correspond to their patch size class from 90ha (black), 270ha, 450ha, 630ha, to 900 ha (light grey)

4. Conclusion

We analyzed the morphological features of fire patches derived from the pixel-level information of 'burn date' delivered by global burned area products, a neglected aspect of these product's quality assessment. Our results confirm earlier findings about the underestimation of burned area from global remote sensing due to small fires omission, but also point out the underestimation of burned area at the patch level as a consequence of a high uncertainty in patch boundary. However, the patch core area derived from global remote sensing seems conservative as well as the general fire shape, a key finding for further analysis of fire regimes and intrinsic processes, and for better DGVM benchmarking.

Acknowledgements: This work was developed within the Fire-Cci project, in the framework of the European Space Agency Climate Change Initiative programme and the IRD/CNPq collaborative agreement project. The Coordenação de Aperfeiçoamento de Pessoal Superior (CAPES, Brazil) provided a PhD grant to Joana Nogueira (BEX-1185-13-6 process). Julien Ruffault was supported by a post-doctoral grant within the European Community's Seventh Framework Program (CLARIS-LPB, Grant Agreement No 212492)

References

Anaya, J.A. and Chuvieco, E. Accuracy assessment of burned area products in the Orinoco basin. **Photogramm. Eng. Remote Sens**. 78(1), 53-60, 2012

Araujo, F. M. and Ferreira, L.G. Satellite base automated burned area detection: a performance assessment of the MODIS MCD45A1 in the Brazilian savanna. **Int. J. Appl. Earth Obs. Geoinf.** 36, 94-102, 2015

Archibald, S. and Roy, D.P. Identifying individual fires from satellite-derived burned area data. Proceedings of the **IEEE International Geoscience and Remote Sensing Symposium**, Cape Town, South Africa, July 2009; pp. III-160-III-163

Barros, A.M.G.; Pereira J.M.C.; Moritz, M.A.; Stephens, S.L. Spatial characterization of wildfire orientation patterns in California. **Forests** 4(1), 197-217, 2013

Bastarrika, A.; Chuvieco, E.; Martin, M. P. Mapping burned areas from Landsat TM/ETM+ data with a two-phase algorithm: Balancing omission and commission errors. **Remote Sens. Environ** 115, 1003–1012, 2011

Bui, R.; Buliung, R.N.; Remmel, T.K. (2012). aspace: A collection of functions for estimating centrographic statistics and computational geometries for spatial point patterns. R package version 3.2

Chuvieco, E. et al. A new global burned area product for climate assessment of fire impacts. **Glob. Ecol. Biogeogr.** 25 (5), 619-629, 2016

Hantson, S.et al. The status and challenge of global fire modelling. **Biogeoscience**s, 13, 3359-3375, 2016

Hijmans, R.J. (2014). raster: raster: Geographic data analysis and modeling. R package version 2.2-31.

Instituto Nacional de Pesquisas Espaciais (INPE). Available online: http:// www.inpe.br/ (accessed on 5 June 2016)

Libonati, R. et al. An algorithm for burned area detection in the Brazilian cerrado Using 4 μm MODIS imagery. **Remote Sens**. 7, 15782-15803 , 2015

Mouillot, F. et al. Ten years of global burned area products from spaceborne remote sensing-A review: Analysis of user needs and recommendations for future developments. **Int. J. Appl. Earth Obs. Geoinf,** 26, 64–79,2014

Oliveira, S.L.J.et al. Ecological implications of fine scale fire patchiness and severity in tropical savannas of northern Australia**. Fire Ecol**. 11(1), 10-31,2015

Padilla, M. et al. Comparing the accuracies of remote sensing global burned area products using stratified random sampling and estimation. **Remote Sens. Environ**. 160, 114-121,2015

Pebesma, E.J.; Bivand, R.S. (2005). Classes and methods for spatial data in R. R News 5 (2)

Randerson, J.T.; Chen, Y.; van der Werf, G.R.; Rogers, B.M.; Morton, D.C. Global burned area and biomass burning emissions from small fires. **J. Geophys. Res.: Biogeosci**. 117, G04012, 21456-2202, 2012

Rothermel, R.C. **A mathematical model for predicting fire spread in wildland fuels.** Res. Pap. INT-115, US Department of Agriculture, Forest Service, Intermountain Forest and Range Experiment Station, Ogden, UT, USA, 1972, 40p, 1972

Roy, D.P. et al. The collection 5 MODIS burned area product – global evaluation by comparison with the MODIS active fire product. **Remote Sens. Environ**. 112 (9), 3690–3707, 2008

Sa, A.C.L; Pereira, J.M.C; Gardner, R.H. Analysis of the relationship between spatial pattern and spectral detectability of areas burned in southern Africa using satellite data. **Int. J. Remote Sensing**. 28: 3583-3601, 2007

Viergever, M. Plano Estadual de Controle de Queimadas e Combate a Incêndios Florestais. Governo do Estado do Tocantins, Brasilia, Brazil, 2009

Vanderwal, J.; Falconi, L.; Januchowski, S.; Shoo, L.; Storlie, C. (2014). SDMTools: Species Distribution Modelling Tools: Tools for processing data associated with species distribution modelling exercises. R package version 1.1-20.

Vilar, L.; Camia, A.; Ayanz, J. S.M. A comparison of remote sensing products and forest fire statistics for improving fire information in Mediterranean Europe. **Eur. J. Remote Sens.,** 48, 345-364, 2015